

## Site-Directed Hydroxyl Radical Probing of the rRNA Neighborhood of Ribosomal Protein S5

Gabriele M. Heilek and Harry F. Noller

Cysteine residues were introduced into three different positions distributed on the surface of ribosomal protein S5, to serve as targets for derivatization with an Fe(II)-ethylenediaminetetraacetic acid linker. Hydroxyl radicals generated locally from the tethered Fe(II) in intermediate ribonucleoprotein particles or in 30S ribosomal subunits reconstituted from derivatized S5 caused cleavage of the RNA, resulting in characteristically different cleavage patterns for the three different tethering positions. These findings provide constraints for the three-dimensional folding of 16S ribosomal RNA (rRNA) and for the orientation of S5 in the 30S subunit, and they further suggest that antibiotic resistance and accuracy mutations in S5 may involve perturbation of 16S rRNA.

Our ignorance of the molecular mechanisms of translation is the result of a lack of detailed knowledge of ribosome structure. This structure has been studied by molecular modeling, based on constraints from phylogenetic, biochemical, and biophysical data (1–3). There is agreement concerning the locations of some features of 16S rRNA in the 30S subunit, whereas others remain controversial (4, 5) because of a lack of sufficient experimental data to constrain the three-dimensional positions of certain regions of 16S rRNA. We are developing a method to provide comprehensive information about the proximities of defined locations on the surfaces of individual ribosomal proteins to individual nucleotides in rRNA, as an alternative to cross-linking and footprinting methods (6, 7). We use Fe(II), chelated by an EDTA linker [1-(*p*-bromoacetamidobenzyl)-EDTA] (BABE) to a specified position on the surface of a single ribosomal protein (8, 9), to generate hydroxyl radicals, which cause localized scission of the RNA backbone (10). As the EDTA linker arm is about 12 Å long, and the hydroxyl radicals have an effective range of about 10 Å, reaction is confined to regions of the RNA within about 22 Å of the linker attachment site. Sites of cleavage are readily identified by primer extension with reverse transcriptase (7). Here we demonstrate the feasibility of this approach, using ribosomal protein S5, whose structure has been determined by x-ray crystallography (11).

Protein S5 is of particular biological interest because it is the target of mutations that confer translational miscoding, cold sensitivity, and resistance to the translational inhibitor spectinomycin (12–14). Although S5 is not among the six 30S subunit proteins that bind 16S rRNA independently (15), footprinting studies of ribonucleo-

protein (RNP) assembly intermediates (16) and cross-linking experiments (17) place S5 in proximity to the RNA near the pseudoknot structure at the convergence of the three major domains of the 16S rRNA secondary structure.

Using site-directed mutagenesis, we introduced cysteines at three different locations on the surface of S5, whose phylogenetic variability (18) suggested that the presence of the Fe(II) probe might not interfere with assembly of the derivatized S5. Position 21 was chosen because of its close proximity to the site of spectinomycin resistance mutations (14), and positions 99 and 129 were chosen because of their proximities to sites of mutations conferring increased amounts of translational miscoding (12). The purified mutant proteins were derivatized with the Fe(II) probe and recon-

stituted with 16S rRNA and mixtures of other 30S ribosomal proteins to yield RNP assembly intermediates containing S5 and seven other proteins, as well as fully assembled 30S ribosomal subunits (19). Sedimentation profiles for the different RNP and 30S constructs were indistinguishable from those assembled from nonderivatized S5. Subunits containing derivatized mutant S5 were as active in binding transfer RNA (tRNA) as were those reconstituted from nonderivatized wild-type S5 (20).

Generation of hydroxyl radicals from Fe(II) tethered to the three different positions of S5 resulted in characteristically different RNA cleavage patterns, which shows that the three sites are located in different RNA environments in both the RNP and 30S subunit constructs (Figs. 1 through 4). When the various constructs were assembled in the presence of excess unmodified S5, the cleavages were not observed, indicating that unmodified S5 competes for assembly of Fe(II)-BABE-S5 (Fig. 2). This control experiment provides additional evidence that Fe(II)-BABE-S5 assembles at the normal S5 binding site. Substantial differences between the observed cleavage patterns of the RNP intermediates and those of the intact 30S subunits suggest that certain RNA structural elements are rearranged during 30S subunit assembly. Cleavages near the 5' end of 16S rRNA were observed in all six constructs, which is consistent with chemical protections by S5 near the 5' terminus (16) and cross-linking of S5 to 16S rRNA at its 5' end and around position 560 (17). Cleavage from the C129-

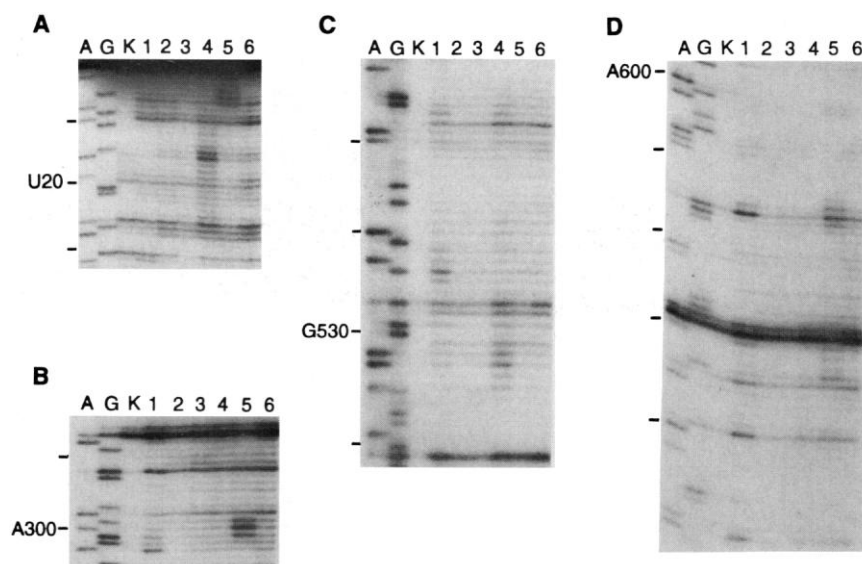


**Fig. 1.** Cleavage of 16S rRNA in RNP particles containing Fe(II) tethered to different positions on protein S5 (42). (A through D) are autoradiographs of gels showing different regions of 16S rRNA. Sites of cleavage were localized by primer extension with reverse transcriptase (7). A and G, sequencing lanes; K, unmodified 16S rRNA. Samples in lanes 1 through 6 were treated with H<sub>2</sub>O<sub>2</sub> and ascorbate. Lane 1, naked 16S rRNA; lane 2, RNP lacking S5; lane 3, RNP with nonderivatized wild-type S5; lane 4, RNP with Fe(II)-C21-S5; lane 5, RNP with Fe(II)-C99-S5; and lane 6, RNP with Fe(II)-C129-S5.

Center for Molecular Biology of RNA, Sinsheimer Laboratories, University of California, Santa Cruz, CA 95064, USA.

linked probe was confined exclusively to the region around the 5' helix. For the C21 and C99 probes, directed cleavage was also observed in several other regions of the RNA.

Cleavages from Fe(II)-Cys<sup>21</sup>-S5 were found in the 3' side of the loop at position 530 and in the nearby bulge loop at position 510 (Fig. 1C, lane 4). These two loops participate in a pseudoknot structure that is important for translational accuracy (21). In the 30S subunit construct, the cleavages near position 530 were intensified, whereas those in the 510 loop disappeared, possibly as a result of protection by protein S12 (16) (Fig. 3, D and E, lane 2). Additional regions of the RNA were cleaved in the Cys<sup>21</sup> 30S subunit construct, but not in the RNP particle, suggesting that these parts of the structure rearrange during later stages of ribosome assembly. Cleavage in the tetraloop at position 420 (Fig. 3C, lane 2), which is also the target of directed hydroxyl radical probing from S4 (22), and near the site of cross-linking of S4 to 16S rRNA (23), is consistent with the proximity of proteins S4 and S5 in the 30S subunit (24). Nucleotides cleaved from C21 in the region of position 915 (Fig. 3G, lane 2) have been footprinted by streptomycin, an error-inducing antibiotic, and contain sites of mutations that confer streptomycin resistance (25).

The Fe(II) probe tethered to C21 is also responsible for cleavage of the RNA around positions 926 and 1400 (Fig. 3, G and J, lane 2), two P-site (the ribosomal binding site for peptidyl-tRNA)-related nucleotides that have been placed in the cleft of the 30S subunit, the site of codon-anticodon interaction (26, 27). These results bear on conflicting reports concerning the distance between the 530 loop and the decoding site (2, 5). The 530 loop has been placed at the opposite side of the 30S subunit from the decoding site by a number of physical and biochemical studies (28). Other evidence, including cross-linking of position 11 of certain mRNA analogs to position 531 (29), has led to the proposal that the 530 loop is located at the decoding site (2). Our data show that both the 530 loop and the 926 and 1400 regions are cleaved by hydroxyl radicals generated from the same position on S5. If the range of hydroxyl radicals and the length of the BABE linker are each about 10 Å, then an estimate of the maximum distance between two nucleotides that are cleaved from the same probing position is  $\pm 20$  Å, or about 40 Å. This distance is considerably less than that found for the 530 loop-decoding site distance ( $>100$  Å), based on the location of S12 in the neutron map as a marker for the 530 loop and S7 for the decoding site (5, 24).

The resolution of this discrepancy is not obvious. Possible explanations include multiple conformations of the 30S subunit or that one or more of the experimental constraints is in error. Further studies will be required to resolve this question.

Fe(II)-Cys<sup>21</sup>-dependent cleavages in the 1055 and 1195 regions (Fig. 3, H and I, lane 2) of the 3' major domain suggest how certain mutations in S5 may confer resistance to the antibiotic spectinomycin (30), an inhibitor of elongation factor G (EF-G)-dependent translocation (31). SpcR mutations have been mapped to positions adjacent to C21 in S5 (11, 30). RNP particles containing the 3' domain of 16S rRNA and its associated proteins, but lacking S5, were

shown to bind spectinomycin with an affinity similar to that of 30S subunits (32), indicating that S5 is not required for spectinomycin binding. Indeed, mutations in 16S rRNA at positions 1066 and 1192 confer a SpcR phenotype (33) and spectinomycin protects the N7 position of G<sup>1064</sup> from attack by dimethyl sulfate (34), suggesting that its binding site includes the G1064-C1192 base pair in the 3' domain of 16S rRNA. Specific cleavage of this region of 16S rRNA by a probe tethered to position 21 of S5 suggests that mutations in S5 could confer spectinomycin resistance by interaction with this region of 16S rRNA as proposed by Ramakrishnan and White (11). Such S5-16S rRNA interactions could also

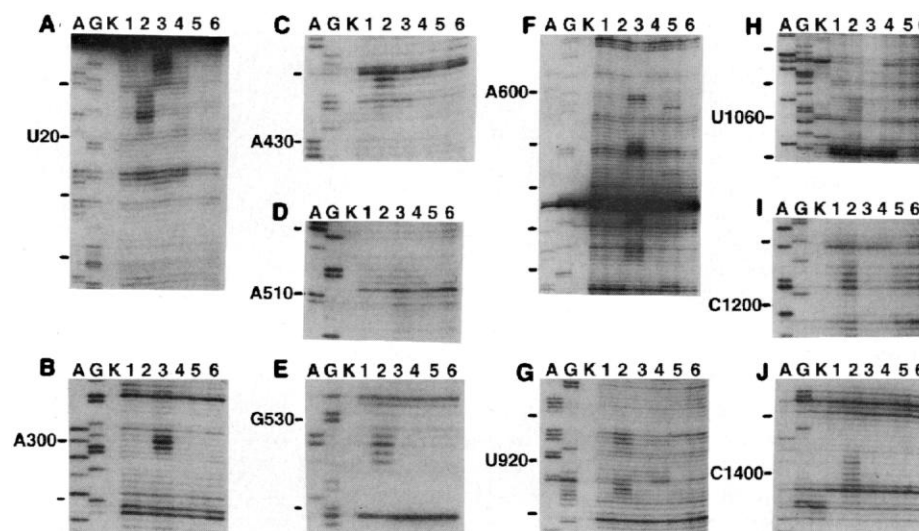
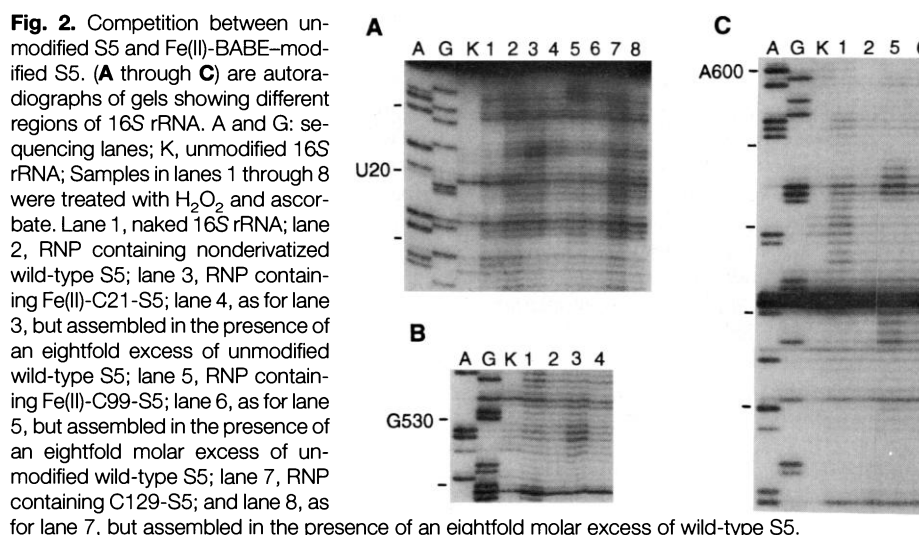


**Fig. 3.** Cleavage of 16S rRNA in 30S subunits containing Fe(II)-S5. (A through J) are autoradiographs of gels showing different regions of 16S rRNA. A and G: sequencing lanes; K, unmodified 16S rRNA. Samples in lanes 1 through 6 were treated with H<sub>2</sub>O<sub>2</sub> and ascorbate. Lane 1, 30S reconstituted with nonderivatized wild-type S5; lane 2, 30S reconstituted with Fe(II)-C21-S5; lane 3, 30S reconstituted with Fe(II)-C99-S5; lane 4, 30S reconstituted with Fe(II)-C129-S5; lane 5, 30S reconstituted with total proteins extracted from 30S ribosomal subunits; and lane 6, natural 30S subunits.

explain why ribosomes lacking S5 are deficient in EF-G-dependent guanosine triphosphatase activity (35).

The C99 probe directs cleavage to distinctly different positions in 16S rRNA, which is consistent with its location at the opposite end of S5 from C21 and C129

(11). One set of hits is in the tetraloop at position 300 (Fig. 3B, lane 3), which is also a target of cleavage from Fe(II) tethered to protein S4 (22), which, along with the cleavages around position 420 from the C21 probe, provide further evidence for the proximity of S4 and S5 in the 30S subunit.

Another target of the C99 probe is in the compound helix located between positions 600 and 640 (Fig. 3F, lane 3) in the central domain (Fig. 4), which has been footprinted by proteins S8 and S16 (16) and cross-linked to S17 (36).

Our data can be used to constrain the rotational orientation of S5 in the 30S subunit. C21 and C99 are at opposite poles of the S5 structure (Fig. 5), and probes attached to these two positions give dramatically different cleavage patterns. Cleavage of the 1055-1190 region by a probe at C21 orients this end of S5 toward the head of the 30S subunit, because this region of the RNA is constrained by proteins S2, S3, S9, and S19, all of which are located in the head of the 30S subunit (24, 37). Cleavage of the distal end of the 620 stem by a probe tethered to C99 orients this end of S5 toward the bottom of the subunit because of interactions of the 620 stem with S8, S16, and S17. The only cleavages that arise from the C129 probe are a limited number of cuts in the 5' helix (Fig. 1A, lane 6; Fig. 3A, lane 4), suggesting that C129 faces away from the RNA, toward the solvent. Figure 5 shows a plausible orientation of S5 in a recent version of our model for the 30S subunit that takes into account the data presented here.

With the use of this same approach to attach probes systematically to surface positions of other ribosomal proteins, it may be possible to obtain sufficient numbers of constraints to determine the structure of the 30S ribosomal subunit directly, at low resolution. In addition, it should be possible to use these constructs to probe the structure of ribosomal RNA (and tRNA and mRNA) in different functional states of the translational cycle. This general strategy should be applicable to the study of any RNP complex, such as the spliceosome, telomerase, and the signal recognition particle.

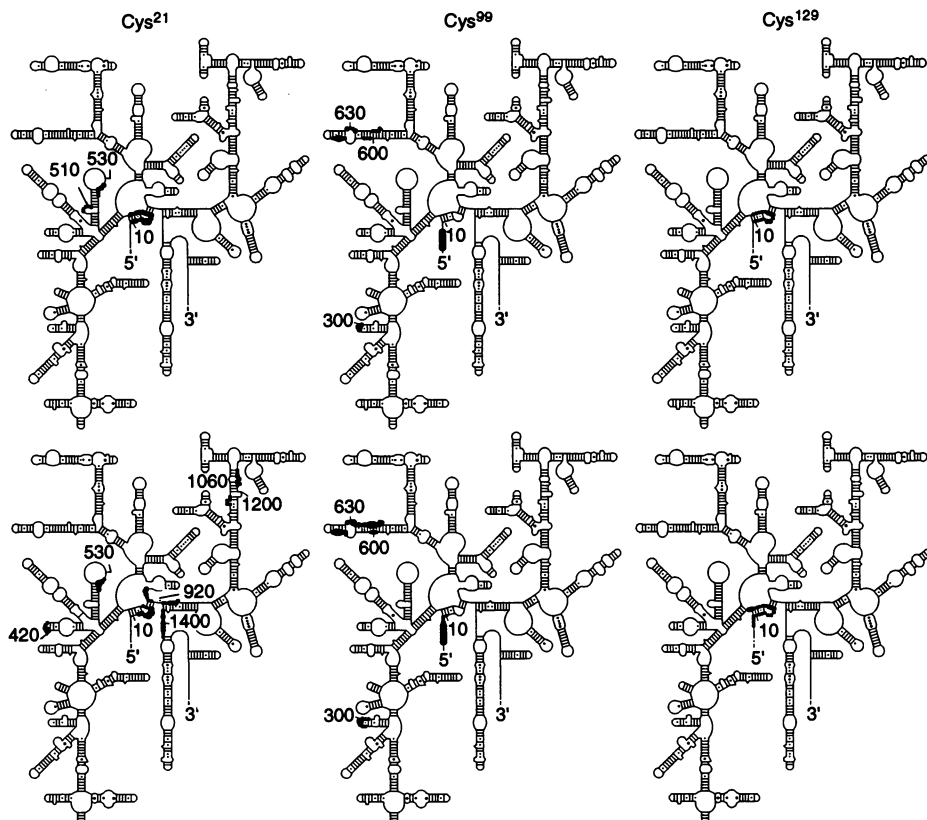
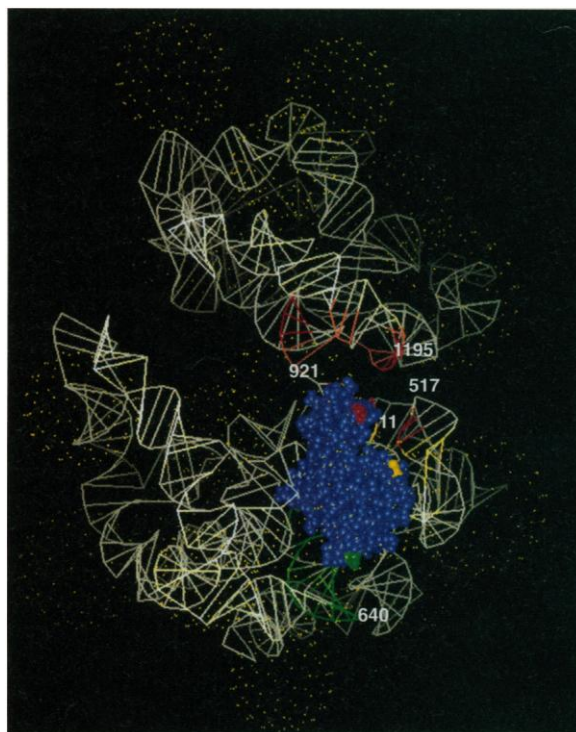


**Fig. 4 (above).** Summary of sites of cleavage of 16S rRNA resulting from Fe(II) tethered to positions 21, 99, and 129 of ribosomal protein S5 incorporated into RNP particles (top) containing 16S rRNA and proteins S4, S7, S8, S15, S16, S17, and S20, and complete 30S ribosomal subunits (bottom).

**Fig. 5 (right).** Positioning of the crystal structure of protein S5 (11) in a recent refinement of a model for the 30S ribosomal subunit (43). S5 is docked on its position as determined by neutron diffraction (24). Positions of cysteines used for tethering of Fe(II) to S5 are indicated in red (Cys<sup>21</sup>), green (Cys<sup>99</sup>), and yellow (Cys<sup>129</sup>), respectively, and the sites of hydroxyl radical cleavage in 16S rRNA are shown in the corresponding colors. The orientation of the model is from the solvent side, with the platform and cleft at the left and the head at the top.



## REFERENCES AND NOTES

1. S. Stern, B. Weiser, H. F. Noller, *J. Mol. Biol.* **204**, 447 (1988).
2. R. Brimacombe, *Eur. J. Biochem.* **230**, 365 (1995);  
\_\_\_\_\_, J. Atmadja, W. Stiege, D. Schüler, *J. Mol. Biol.* **199**, 115 (1988).
3. A. Malhotra and S. C. Harvey, *J. Mol. Biol.* **240**, 308 (1994).
4. R. Brimacombe, *Biochimie* **74**, 319 (1992).
5. T. Powers and H. F. Noller, *Trends Genet.* **10**, 27 (1994).
6. R. Brimacombe et al., in *The Ribosome: Structure, Function and Evolution*, W. E. Hill et al., Eds. [American Society for Microbiology (ASM), Washington, DC, 1990], pp. 93-106.
7. S. Stern, D. Moazed, H. F. Noller, *Methods Enzymol.* **164**, 481 (1988).
8. L. H. DePiemer, C. F. Meares, D. A. Goodwin, C. J. Diamanti, *J. Labelled Compd. Radiopharm.* **18**, 1517 (1981).
9. T. M. Rana and C. F. Meares, *Proc. Natl. Acad. Sci. U.S.A.* **88**, 10578 (1991).
10. D. W. Celander and T. R. Cech, *Biochemistry* **29**, 1355 (1990).

11. V. Ramakrishnan and S. W. White, *Nature* **358**, 768 (1992).
12. W. Piepersberg, A. Böck, H. G. Wittmann, *Mol. Gen. Genet.* **140**, 91 (1975).
13. C. Guthrie and M. Nomura, *Proc. Natl. Acad. Sci. U.S.A.* **63**, 384 (1969).
14. W. Piepersberg, A. Böck, M. Yaguchi, H. G. Wittmann, *Mol. Gen. Genet.* **143**, 43 (1975).
15. W. A. Held, B. Ballou, S. Mizushima, M. Nomura, *J. Biol. Chem.* **249**, 3103 (1974).
16. S. Stern, T. Powers, L. M. Changchien, H. F. Noller, *J. Mol. Biol.* **201**, 683 (1988).
17. M. Osswald et al., *Nucleic Acids Res.* **15**, 3221 (1987).
18. S. Mian and H. F. Noller, unpublished material.
19. The gene for ribosomal protein S5 (38) was cloned by polymerase chain reaction from total *Escherichia coli* MRE600 genomic DNA, and cysteines were created at positions 21, 99, and 129 of S5 by site-directed mutagenesis (39). Mutant and wild-type genes were placed downstream from a T7 promoter in pET-11a (40) and overexpressed in *E. coli* DH5a. S5 proteins were purified by chromatography on a Pharmacia Resource S fast protein liquid chromatography column with the use of a 50 to 300 mM sodium acetate (NaOAc) (pH 5.6) gradient in 6 M urea at 4°C. Ribosomes, 30S ribosomal subunits, and 16S rRNA were isolated as described previously (41). A complex between BABE and Fe(II), prepared as described previously (8), was conjugated with mutant S5 proteins by mixing of 20  $\mu$ l of a 50  $\mu$ M solution of S5 [in 80 mM K-Hepes (pH 7.7), 1 M KCl, and 6 mM  $\beta$ -mercaptoethanol] with 10  $\mu$ l of a 10 mM solution of Fe-BABE in a buffer containing 1 M KCl, 80 mM Hepes (pH 7.7), and 0.01% Nikkol (Nikko Chemicals, Tokyo, Japan), in a volume of 100  $\mu$ l, followed by incubation at 37°C for 15 min. Modified S5 was separated from excess reagent with Microcon3 vials (Amicon, Tokyo, Japan), in a volume of 100  $\mu$ l, followed by incubation at 37°C for 15 min. Modified S5 was separated from excess reagent with Microcon3 vials (Amicon). Complexes between S5 or Fe(II)-derivatized S5 and 16S rRNA were formed, in a typical experiment, by adding 20 pmol of *E. coli* 16S rRNA [in 50 mM tris-HCl (pH 7.5), 20 mM MgCl<sub>2</sub>, and 300 mM KCl] to buffer A [80 mM K-Hepes (pH 7.7), 20 mM MgCl<sub>2</sub>, and 0.01% Nikkol]. After addition of 2.7  $\mu$ l of a 30  $\mu$ M solution of S5 or Fe(II)-derivatized S5 and 2  $\mu$ l of a 40  $\mu$ M mixture containing proteins S4, S7, S8, S15, S16, S17, and S20 [all proteins were stored in 80 mM K-Hepes (pH 7.7), 1 M KCl, and 6 mM  $\beta$ -mercaptoethanol], the salt concentration was adjusted to 330 mM to give a final reaction volume of 50  $\mu$ l. Incubation took place at 40°C for 1 hour, followed by 10 min on ice. Reconstitution of 30S ribosomal subunits containing Fe(II)-derivatized S5 or unmodified S5 was done similarly, except that 10  $\mu$ l of an 8  $\mu$ M solution of  $\Sigma$ -S5 (a mixture containing all 30S ribosomal proteins except S5) was used to allow formation of complete subunits. S5-16S rRNP complexes and reconstituted 30S subunits were purified by sedimentation in a SW41 rotor for 18 hours at 35,000 rpm at 4°C, with the use of a 10 to 40% sucrose gradient in 50 mM tris-HCl (pH 7.5), 20 mM MgCl<sub>2</sub>, and 100 mM KCl.
20. Poly(U)-dependent binding of tRNA<sup>Phe</sup>, performed as described (26), was used as an assay for the activity of reconstituted 30S subunits.
21. C. R. Woese and R. R. Gutell, *Proc. Natl. Acad. Sci. U.S.A.* **86**, 3119 (1989); T. Powers and H. F. Noller, *EMBO J.* **10**, 2203 (1991).
22. G. Heilek, R. Marusak, C. F. Meares, H. F. Noller, *Proc. Natl. Acad. Sci. U.S.A.* **92**, 1113 (1995).
23. C. Zwieb and R. Brimacombe, *Nucleic Acids Res.* **5**, 1189 (1978).
24. M. S. Capel et al., *Science* **238**, 1403 (1987).
25. P. E. Montandon, R. Wagner, E. Stutz, *EMBO J.* **6**, 3705 (1986).
26. D. Moazed and H. F. Noller, *Cell* **47**, 985 (1986); U. von Ahlsen and H. F. Noller, *Science* **267**, 234 (1995).
27. M. I. Oakes, M. W. Clark, E. Henderson, J. A. Lake, *Proc. Natl. Acad. Sci. U.S.A.* **83**, 275 (1986).
28. L. S. Lasater, L. Montessano-Roditis, P. A. Cann, D. G. Giltz, *Nucleic Acids Res.* **18**, 477 (1990); A. Scheinmann et al., *Biochimie* **74**, 307 (1992); M. R. Trempe, K. Ohgi, D. G. Giltz, *J. Biol. Chem.* **257**, 9822 (1982).
29. J. Rinke-Appel, N. Jünke, K. Stade, R. Brimacombe, *EMBO J.* **10**, 2195 (1991).
30. B. Matkovic, A. Herzog, A. Bollen, L. Topisirovic, *Mol. Gen. Genet.* **179**, 135 (1980).
31. N. Bilgin, A. A. Richter, M. Eherenberg, A. E. Dahlberg, C. G. Kurland, *EMBO J.* **9**, 735 (1990).
32. R. R. Samaha, B. O'Brien, T. W. O'Brien, H. F. Noller, *Proc. Natl. Acad. Sci. U.S.A.* **91**, 1884 (1994).
33. C. D. Sigmund, M. Ettayebi, E. A. Morgan, *Nucleic Acids Res.* **12**, 4653 (1984); U. Johanson and D. Hughes, *ibid.* **23**, 464 (1995).
34. D. Moazed and H. F. Noller, *Nature* **327**, 389 (1987).
35. R. C. Marsh and A. Parmeggiani, *Proc. Natl. Acad. Sci. U.S.A.* **70**, 151 (1973).
36. A. Kyriatsoulis et al., *Nucleic Acids Res.* **14**, 1171 (1986).
37. M. I. Oakes, A. Scheinmann, T. Atha, G. Shankweiler, J. A. Lake, in *The Ribosome: Structure, Function and Evolution*, W. E. Hill et al., Eds. (ASM, Washington, DC, 1990), pp. 180-193; M. Stöffler-Meilicke and G. Stöffler, *ibid.*, pp. 123-133.
38. D. P. Ceretti, D. Dean, G. R. Davis, D. M. Bedwell, M. Nomura, *Nucleic Acids Res.* **11**, 2599 (1983).
39. T. A. Kunkel, *Proc. Natl. Acad. Sci. U.S.A.* **82**, 488 (1985).
40. F. W. Studier, A. H. Rosenberg, J. J. Dunn, J. W. Dubendorff, *Methods Enzymol.* **185**, 61 (1990).
41. D. Moazed, S. Stern, H. F. Noller, *J. Mol. Biol.* **187**, 399 (1986).
42. Formation of hydroxyl radicals was initiated by addition of 1  $\mu$ l of 250 mM ascorbic acid and 1  $\mu$ l of 2.5% H<sub>2</sub>O<sub>2</sub> to 25  $\mu$ l of a solution of Fe(II)BABE-S5 RNP complex (0.2 mg/ml) in buffer A containing 330 mM KCl, or to 25  $\mu$ l of a solution of Fe(II)BABE-S5 30S subunits (0.32 mg/ml), followed by incubation for 10 min at 4°C. The reaction was terminated by addition of 1/10 volume 3 M NaOAc (pH 5.2), 1  $\mu$ l of a solution of glycogen (10 mg/ml), and 2.5 volume ethanol. The modified RNA was extracted and analyzed by primer extension as described (7).
43. H. F. Noller, T. Powers, G. M. Heilek, S. Mian, B. Weiser, unpublished data.

22 November 1995; accepted 7 March 1996

## Activation of Gal4p by Galactose-Dependent Interaction of Galactokinase and Gal80p

F. T. Zenke, R. Engels, V. Vollenbroich, J. Meyer, C. P. Hollenberg, K. D. Breunig\*

Yeast galactokinase (Gal1p) is an enzyme and a regulator of transcription. In addition to phosphorylating galactose, Gal1p activates Gal4p, the activator of *GAL* genes, but the mechanism of this regulation has been unclear. Here, biochemical and genetic evidence is presented to show that Gal1p activates Gal4p by direct interaction with the Gal4p inhibitor Gal80p. Interaction requires galactose, adenosine triphosphate, and the regulatory function of Gal1p. These data indicate that Gal1p-Gal80p complex formation results in the inactivation of Gal80p, thereby transmitting the galactose signal to Gal4p.

Gal4p, the key regulator of galactose metabolism in yeast, is a prototypical transcriptional activator that functions in fungal, plant, and animal cells (1). Genetic analysis revealed that the activity of Gal4p is controlled by the inhibitory protein Gal80p, and this system became a model to study eukaryotic gene regulation. However, it has been unclear how induction by galactose relieves the inhibitory effect of Gal80p on Gal4p activation function. Signal transmission requires the function of either the *GAL3* or the *GAL1* gene product. *GAL1* encodes galactokinase (Gal1p), the first enzyme of galactose metabolism. Gal3p shows homology to Gal1p but lacks galactokinase activity (2, 3). Early models proposing that both proteins catalyze the conversion of galactose into an inducer molecule that binds to and inactivates Gal80p [reviewed in (4)] have recently been questioned (3, 5).

The yeast *Kluyveromyces fragilis* shares the regulatory mechanisms controlling expression of the galactose regulon with *Saccharomyces cerevisiae*. The transcriptional activator KIGal4p (also named Lac9p) and its

inhibitor KIGal80p are exchangeable with their *S. cerevisiae* counterparts (6, 7). However, induction of galactose as well as lactose metabolism is entirely dependent on *K. lactis* Gal1p (KIGal1p) because *K. lactis* lacks a functional *GAL3* homolog. We have previously shown that induction requires a regulatory function of KIGal1p that is independent of the galactokinase activity and that complements a *S. cerevisiae* *gal3* mutation (8, 9).

Because in *K. lactis* Gal1p is only required for induction in the presence of Gal80p (10), we investigated whether KIGal1p inactivates Gal80p directly. Using a biochemical approach, we assayed for the formation of a complex between the two proteins. We tagged KIGal80p with six His residues (<sup>His</sup>KIGal80p) (11) and then enriched the tagged protein from *K. lactis* cell extracts by binding to Ni-nitrilo-tri-acetic acid (NTA)-agarose (12). Protein immunoblot analysis with a polyclonal antiserum to KIGal80p (anti-KIGal80p) demonstrated that the epitope-tagged KIGal80p bound specifically to Ni-NTA-agarose (Fig. 1A). Cell extracts containing either of the two proteins, <sup>His</sup>KIGal80p or KIGal1p, were analyzed in binding assays as controls. Only when both protein extracts were mixed could KIGal1p be detected among the Ni-

Institut für Mikrobiologie, Heinrich-Heine-Universität Düsseldorf, Universitätsstrasse 1 D-40225 Düsseldorf, Germany.

\*To whom correspondence should be addressed.